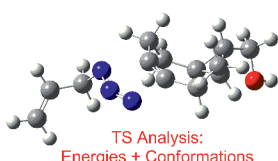
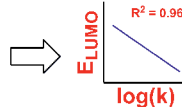


Activation energies, distortion energies, and TS conformational data were compared in a set of strained cyclooctynes in strain-promoted azide-alkyne cycload-



TS Analysis:
Energies + Conformations



dition (SPAAC) reactions. Only electronic effects could be accurately related to experimental rate data.

Strained Molecules in Cycloaddition

J. Garcia-Hartjes, J. Dommerholt,
T. Wennekes, F. L. van Delft,
H. Zuilhof* 1–10

Electronic Effects versus Distortion Energies During Strain-Promoted Alkyne-Azide Cycloadditions: A Theoretical Tool to Predict Reaction Kinetics



Keywords: Reaction mechanisms / Ab initio calculations / Cycloaddition / Click chemistry / Strained molecules / Alkynes

DOI: 10.1002/ejoc.201201627

Electronic Effects versus Distortion Energies During Strain-Promoted Alkyne-Azide Cycloadditions: A Theoretical Tool to Predict Reaction Kinetics

Jaime Garcia-Hartjes,^[a] Jan Dommerholt,^[b] Tom Wennekes,^[a] Floris L. van Delft,^[b] and Han Zuilhof^{f*[a,c]}

Keywords: Reaction mechanisms / Ab initio calculations / Cycloaddition / Click chemistry / Strained molecules / Alkynes

Second-order reaction kinetics of known strain-promoted azide-alkyne cycloaddition (SPAAC) reactions were compared with theoretical data from a range of ab initio methods. This produced both detailed insights into the factors determining the reaction rates and two straightforward theoretical tools that can be used to predict a priori the reaction kinetics of novel cyclooctynes for strain-promoted cycloaddition reactions. Multiple structural and electronic effects contribute to the reactivity of various cyclooctynes. It is therefore hard to

relate a physical or electronic property directly and independently to the reactivity of the cyclooctyne. However, we show that Hartree-Fock LUMO energies, which were acquired while calculating activation energies at the MP2 level of theory, correlate with second-order kinetic rate data and are therefore usable for reactivity predictions of cyclooctynes towards azides. Using this correlation, we developed a simple theoretical tool that can be used to predict the reaction kinetics of (novel) cyclooctynes for SPAAC reactions.

Introduction

The strain-promoted azide-alkyne cycloaddition (SPAAC) reaction is increasingly applied for bio-orthogonal purposes. Cyclooctynes have proven valuable because of their relative biological inertness and their strain-induced high efficiency, and selectivity towards azides in cycloaddition reactions.^[1] Unlike in the copper-catalyzed variant of Huisgen's 1,3-dipolar cycloaddition,^[2] i.e., the copper-catalyzed azide-alkyne cycloaddition (CuAAC), which emerged over the years as the prototypical "click reaction",^[3] there is no need for toxic additives such as Cu^I. This is advantageous because copper ions can induce undesirable side-reactions such as non-specific binding to thiol-groups and oxidative damage that both Cu^I and Cu^{II} ions are able to inflict on biomolecules.^[4] Furthermore, because cyclooctynes are generally not reactive towards other cellular components in aqueous media, they can be used in studies on the cellular level.^[5]

In 1953, Blomquist,^[6] and later Wittig and Krebs,^[7] described the reaction of cyclooctyne (OCT, **1**; Figure 1) with phenyl azide as an "explosive reaction". Based on work by

Turner et al.^[8] on the ΔH of hydrogenation of unsaturated aliphatic compounds (including cyclooctyne), Bertozzi later assigned significant rate enhancements to the ring strain of 18 kcal/mol^[9] for **1** compared with unstrained alkynes. Subsequently, the use of electron-poor cyclooctynes was shown to speed up the reaction significantly, specifically in 3,3-difluorocyclooct-1-yne (DIFO, **2**).^[5d,10] Some of us developed bicyclo[6.1.0]non-4-yne (BCN, **3**)^[11] with the additional advantage over earlier cyclooctynes that it is readily prepared and symmetrical, thus avoiding the formation of regioisomeric adducts upon cycloaddition with an organic azide (Figure 2). Apart from electron-withdrawing groups, such as the fluorine groups in compound **2**, the addition of extra ring strain was also shown to be advantageous, as for example implied from the observed high rates for the reaction with 3,7-dibenzocyclooctyne (DIBO) **4**.^[13] In 2010, difluorobenzocyclooctyne (DIFBO) was described,^[14] which combines the electron-withdrawing effect of the fluorine atoms of **2** with the ring strain of **4**. This compound was shown to be the most rapidly reacting cyclooctyne towards azides reported to date, but was not taken up in the current study because of its lack of stability outside a protective cyclodextrin shell. Based on the framework of **4**, two endocyclic nitrogen-containing dibenzocyclooctyne derivatives have been published that contain either a CH₂ group and a nitrogen atom in the ring (DIBAC, **5**),^[15,16] or an endocyclic amide (lactam) functionality and no saturated carbon atoms in the cyclooctyne ring (BARAC, **6**).^[17] Kinetic data are available for **2–6** (Table 1), and for an analogue of **1** that contains an alkoxy moiety at the 3-position.^[9] Compound **7** was described in the literature,^[12] but not in reaction with azides. Compounds **8–10** are strained models that, to the

[a] Laboratory of Organic Chemistry, Wageningen University, Dreijenplein 8, 6703 HB, Wageningen, The Netherlands
E-mail: Han.Zuilhof@wur.nl
Homepage: www.wageningenur.nl/orc

[b] Institute of Molecules and Materials, Radboud University Nijmegen, Heijendaalseweg 135, 6525 AJ, Nijmegen, The Netherlands

[c] Department of Chemical and Materials Engineering, King Abdulaziz University, Jeddah, Saudi Arabia

Supporting information for this article is available on the WWW under <http://dx.doi.org/10.1002/ejoc.201201627>.

Strain-Promoted Alkyne-Azide Cycloadditions

best of our knowledge, have not been described in literature at the time of writing.

Relatively little theoretical work has been published that correlates experimental and calculated data of these strain-promoted cycloadditions. Various properties are known to influence the reaction kinetics of these cyclooctynes in SPAAC reactions (Figure 3). For example, Houk and co-workers performed B3LYP/6-31G(d) optimizations to compare the reactivity of **1** and **2**,^[19] which were more recently

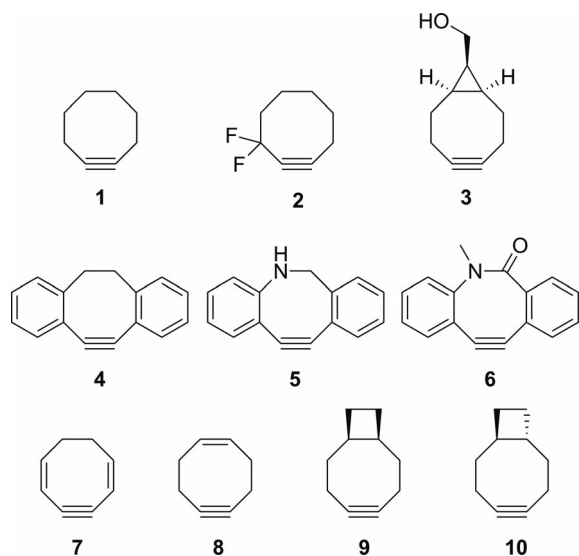


Figure 1. Cyclooctynes under study.

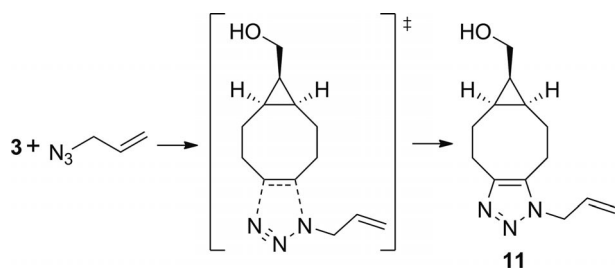


Figure 2. SPAAC of strained cyclooctyne BCN (**3**) and allyl azide, yielding triazole **11**.

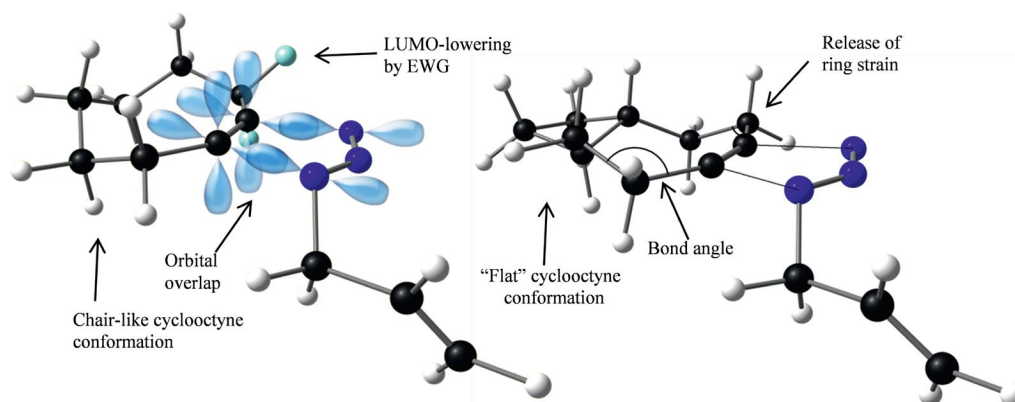


Figure 3. TS conformation of DIFO (**2**) (left) and *trans*-cyclobutyl-substituted **10** (right) with allyl azide, with focus on the various properties of the cyclooctynes that influence their SPAAC reaction kinetics.

Table 1. Experimental data of SPAAC second-order reaction kinetics of cyclooctynes with benzyl azide.

Compd.	k [$\cdot 10^{-3} \text{ M}^{-1} \text{ s}^{-1}$]	Solvent	Ref.
1	5.8	CD ₃ CN/D ₂ O	[a]
2	76	CH ₃ CN	[5d]
3	140	CD ₃ CN/D ₂ O	[11]
4	170	CD ₃ OD	[13]
	120	CD ₃ CN	[18]
5	310	CD ₃ OD	[15]
6	960	CH ₃ CN	[17]

[a] Current work; see the Supporting Information for details.

complimented with a more extensive series of SCS-MP2/6-311G(d) single-point computations on B3LYP-optimized geometries.^[20] These studies concluded that the difference in the reactivity of various cyclooctynes is based on the difference in distortion energies of the alkynes, which is required to deform it from the reactant geometry to the geometry it has in the transition state (TS). In addition, the ring strain in cyclooctynes has been investigated systematically by Bach with B3LYP/6-311+G(3df,2p) calculations.^[21] He calculated that the barrier for cycloaddition of the benzyl azide and DIFO (**2**) is 2.3 kcal/mol lower than addition to **1** (Figure 4). This method was also used to investigate the trends in activation barriers for the 1,3-dipolar cycloadditions of azides with various cyclooctynes, dibenzocyclooctynes, and azacyclooctynes. Subsequently, Goddard and co-workers concluded that suitable placement (e.g., on the position next to the *sp*-hybridized alkyne carbons) of electron-withdrawing substituents leads to LUMO-lowering effects on the alkyne, and that this is accompanied by higher reactivity of cyclooctynes towards cycloaddition with azides.^[22] Houk et al. showed an approximately 2 kcal/mol increase in reactivity of **2** with respect to the parent compound **1**. Gold et al. confirmed this finding and elaborated with Natural Bond Order (NBO) analysis that hyperconjugative donation of the alkyne π -system to the $\sigma^* \text{C-F}$ orbital directly leads to the TS stabilization through the assistance in alkyne bending,^[23] which, together with the LUMO-lowering effect described by Goddard earlier, is the apparent driving force for the 50-fold increase of reactivity

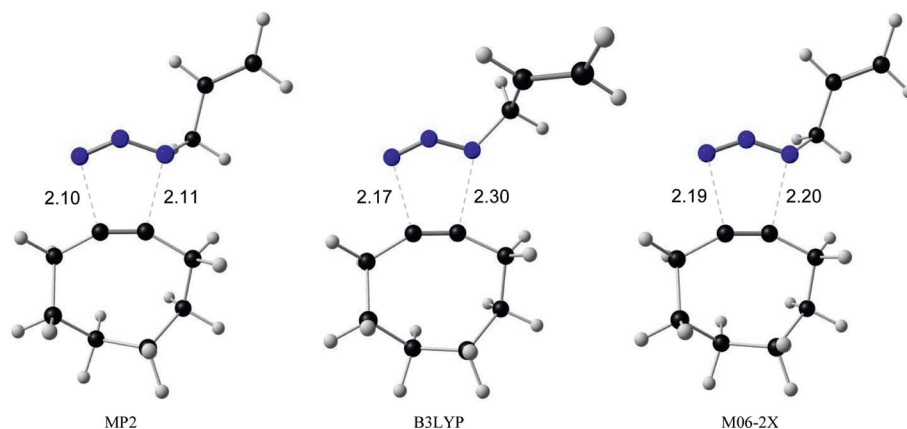


Figure 4. TS conformations of **1** and allyl azide, calculated with MP2, B3LYP, and M06-2X, respectively.

of **2**. Both Gold and Goddard supported the strategy of lowering the energy of the TS to increase reactivity towards azides rather than reactant destabilization. In case of **2**, increased reactivity is a direct result of E_a lowering. Gold hinted at a theoretical tool that could be developed to predict reactivity in the form of a combination of the calculable molecule properties described above. Recently, the reaction kinetics of BARAC (**6**) derivatives were shown to vary depending on the addition of several substituents.^[24] The reaction kinetics of the derivatives were subsequently compared with the results of B3LYP/6-31G(d) calculations. It was found that addition of fluorine groups on the aryl groups of BARAC (**6**), resulted in an increase in reactivity of ca. 75% compared with its parent compound **6**. On the basis of B3LYP calculations, this was attributed to increased stabilizing interaction energy in the TS. In the same study, a decrease in the alkyne bond angle was correlated to an increase in reactivity. The authors suggested that the calculated TS distortion and interaction energies could be used in the design of novel cyclooctynes. To date, however, a generally applicable computational tool that can be used to correlate the structures of these cyclooctynes to their reaction kinetics, has not yet been described.

In the current paper, we will focus in more detail on the transition states of SPAAC reactions, and describe tools that predict a priori the reaction kinetics of novel cyclooctynes for application in these cycloaddition reactions. Given the still growing interest in SPAAC reactions, it is highly desirable to have a simple theoretical tool that can predict the reactivity of novel, hypothetical cyclooctynes. Until now, researchers have mainly focused on the development of faster reacting cyclooctynes. However, the cost of increased reactivity often paid by decreased stability. This is, for example, seen in DIBO (**4**),^[13] which needs to be stored while deprived of light and oxygen. The decreased stability of highly reactive cyclooctynes hampers the further development of SPAAC reactions in material sciences such as, in our own experience, the development of biosensors.^[26] Furthermore, these compounds with a high intrinsic energy are prone to lose their selective reactivity by also being able

to undergo – in addition to SPAAC reactions – for example, a thiol-yne reaction with cysteines, which would complicate the application of these cyclooctynes in biosciences. The ability to tune the reactivity of cyclooctynes by combining an increase in reactant stability with a high efficiency during SPAAC, is therefore of paramount importance in both biological and material sciences.^[25] Hence, it would be advantageous if the design of novel cyclooctynes with, for example, extra groups that increase the water solubility, could be guided by predicting their reactivity before embarking on a resource-consuming synthetic undertaking.

We here present precisely this: a theoretical tool that can be used to accurately predict SPAAC reaction kinetics. Furthermore, we describe an even simpler, albeit less accurate, tool that can be used by non-theoreticians that only requires a ChemDraw-like chemical structure as input to quickly give an indication of the reactivity of new cyclooctynes before they are actually developed. In the study presented here, we further elucidate the relationship between SPAAC kinetics and cyclooctyne electronic properties, by investigating the SPAAC transition state structures and energies for a structurally diverse set of ten cyclooctynes (**1–10**; Figure 1). This was performed with a combination of DFT (B3LYP,^[27] M06-2X^[28]) and SCS-MP2^[29] calculations. Among the ten selected cyclooctynes, six (**1–6**) have been previously used in SPAAC reactions and four (**7–10**) have not yet been used. Finally, to improve the benchmarking of our calculations, additional competition experiments and kinetic constant determinations were performed on cyclooctynes **1–3**.

Computational and Experimental Methods

Calculations were performed using the Gaussian 09 set of programs.^[30] Structures (reactants and transition states) were optimized, and the resulting geometries were shown to be real minima or transition states on the potential energy surface by vibrational frequency computations. The standard IEFPCM dielectric continuum solvent model for

MeOH with UA0 radii was used. Optimization was consistently performed using the 6-311G(d,p) basis set, at the B3LYP, M06-2X, and MP2 levels of theory. Following the optimization, single-point energies were obtained by using the 6-311+G(2d,2p) basis set for all these three methods, while for the MP2-optimized geometries SCS-MP2 energies were obtained.^[29b] Zero-point energies were included in all values. Geometries and vibrations were visualized using Gaussview 4. The syntheses of **1** and allyl azide were performed as described in the Supporting Information. Determination of the reaction kinetics of unsubstituted cyclooctyne (**1**) with benzyl azide was performed according to the literature,^[11] as described in detail in the Supporting Information. Competition experiments of **1**, benzyl azide and allyl azide were performed as described in the Supporting Information.

Results and Discussion

Alkyne-Azide Cycloadditions

Table 2 depicts the activation energies obtained from calculations with B3LYP, M06-2X, and SCS-MP2 methods for the ten cyclooctynes under investigation. Because all compounds clearly contain strain, triple- ζ [6-311G(d,p)] basis sets were employed for the optimizations, whereas the single-point energy calculations involved the flexible 6-311+G(2d,2p) basis sets. From experimental studies on reaction kinetics, it is well-known that **3** reacts appreciably faster than **2** and at least an order of magnitude faster than **1** (Table 1). Originally, **1** was published including an alkoxy substituent on the 3-position.^[9] The second-order rate constant was also published for this compound ($k = 2.4 \times 10^{-3} \text{ M}^{-1} \text{ s}^{-1}$) but considering that the 3-substituent may induce both steric and electronic effects on the reaction, we decided not to use this data in the comparison with the calculated activation energy. Therefore, **1** was synthesized (see the Supporting Information for experimental details), and its second-order rate constant in the SPAAC reaction with benzyl azide was determined to be $k = 5.8 \times 10^{-3} \text{ M}^{-1} \text{ s}^{-1}$ in $\text{CD}_3\text{CN}/\text{D}_2\text{O}$ (3:1). All currently available kinetic data for the reaction of cyclooctynes **1–6** and azides are presented in Table 1, and range over more than two orders of magnitude. The approximate order of experimental reactivity of these compounds in various media is $6 > 5 > 4 \approx 3 > 2 > 1$. This order was, however, not borne out by B3LYP-based calculations, which yielded a relative order of $2 > 1 > 6 > 3 > 5 > 4$. To check whether this discrepancy could be remedied by the use of another DFT functional, while keeping the computational advantage of the relatively fast density functional theory, Truhlar's M06-2X functional was employed. However, the M06-2X functional was also unable to reproduce a qualitative trend that was consistent with the experimental observation, and yielded a rate order $6 > 5 \approx 2 > 1 \approx 3 > 4$. In contrast, MP2 calculations did follow the order of reactivity (see the Supporting Information, Figure S6), but produced incorrect, negative, activation energies. When, however, scaled to

Table 2. Calculated activation energies (kcal mol^{-1}) in the gas phase and in MeOH (IEFPCM solvent model), of the SPAAC reaction for the studied cyclooctynes with allyl azide (**A**) or benzyl azide (**B**) obtained by SCS-MP2, B3LYP, and M06-2X calculations.

Compd.	SCS-MP2		B3LYP		M06-2X	
	Gas	MeOH	Gas	MeOH	Gas	MeOH
1 + A	10.5	11.3	12.1	13.2	11.8	13.0
1 + B	9.6	10.5	11.9	9.8.2	11.1	12.7
2 + A ^[a]	6.7	6.4	11.5	11.6	9.4	9.7
2 + B ^[a]	6.3	6.0	11.6	11.9	9.6	9.9
3 + A	6.5	7.4	13.0	14.1	11.7	12.9
3 + B	6.2	7.1	n.d. ^[b]		n.d. ^[b]	
4 + A	6.3	7.7	16.5	17.9	12.3	13.9
4 + B	5.7	7.7	15.0	11.6	11.5	13.4
5 + A	3.5	5.2	13.7	15.4	9.4	11.2
6 + A	2.1	3.5	12.9	14.5	7.7	9.5
7 + A	5.7	6.3	12.0	12.9	10.8	11.6
7 + B	5.4	5.9	12.1	7.9	10.8	11.8
8 + A	8.6	9.5	13.8	15.1	12.6	14.1
9 + A	7.5	8.7	13.3	14.6	12.2	13.8
10 + A	9.6	10.7	15.2	16.5	12.6	14.1

[a] Only 1,4-addition (*trans*) transition states were calculated.
[b] n.d.: nNot determined.

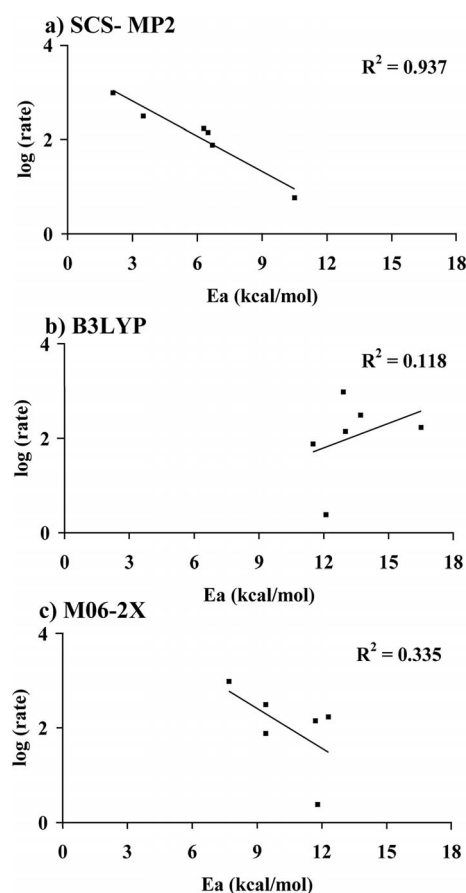


Figure 5. Plot of the logarithm of experimental second-order rate constants (see Table 1 for references) versus calculated activation energies obtained from (a) SCS-MP2/6-311+G(2d,2p)//MP2/6-311G(d,p); (b) B3LYP/6-311+G(2d,2p)//B3LYP/6-311G(d,p), and (c) M06-2X/6-311+G(2d,2p)//M06-2X/6-311G(d,p) calculations.

SCS-MP2 (Figure 5, a), the calculations could properly mimic the complete experimental trend in relative reactivities and also produced realistic activation energies (Table 2). For example, it was clear from these calculations that **6** was the fastest in reacting azides and **1** was the slowest.

Application of this method to compounds **7–10** confirmed the role of ring strain in determining the height of the SPAAC activation energy barrier. Increasing the cyclooctyne ring strain in **7** and **8** by inclusion of sp^2 -hybridized carbon atoms was predicted to lead to a significantly increased reactivity towards cycloaddition with azides compared with **1**. Comparison of compound **7** with **4** revealed that an increased size of the conjugated system also plays an important role in lowering the activation energy barrier. Both **7** and **4** have similar ring strain, but the latter has a more extended π -electron system. In addition to the ring strain and size of the conjugated system, conformational stabilities also affect the cyclooctyne reactivity. For example, the *trans*-cyclobutyl moiety in **10** restricts the eight-membered-ring conformation to a flattened structure (Figure 3). This impedes the formation of the chair-like conformation that the eight-membered ring in cyclooctynes preferentially adopts in the TS of SPAAC reactions, as is shown for **2**. The analogous *cis*-cyclobutyl-containing compound **9** adopts a chair conformation and is correspondingly cal-

culated to be more reactive than **10** (see Table 2, and the Supporting Information, Figure S7 for TS geometries).

Transition State Activation Energies

Figure 5 shows plots of the logarithm of experimental second-order rate constants against the calculated activation energies as obtained by SCS-MP2, B3LYP, and M06-2X calculations. Clearly, the correlations of the experimental rate constants with B3LYP data ($R^2 = 0.118$) and M06-2X data ($R^2 = 0.335$) are insufficient to be used in predicting the reaction kinetics of novel cyclooctynes. Given the significant differences in TS geometries (see Figure 5), doubts arise concerning the use of DFT-derived geometries for single-point activation energy determinations. In contrast, when the experimental rate constants were plotted against SCS-MP2 calculated activation energies, using MP2-derived geometries in the gas phase, a clear linear relation with good correlation was found ($R^2 = 0.937$). The correlation was lower between the SCS-MP2 activation energies in MeOH and the experimental rate constants (see the Supporting Information, Figure S8). The solvent model used, however, only provides a rough approximation of the complex interactions between MeOH and molecules in the

	OCT (1)	$\angle N_3$	138.0°	$d N^{\text{term}}-C^1$	2.10 Å
		$\angle C^1-C^2-CH_2$	150.0°	$d N^{\text{int}}-C^2$	2.11 Å
		$\angle C^2-C^1-CH_2$	153.2°	$d C\equiv C$	1.25 Å
	DIFO (2)	$\angle N_3$	137.5°	$d N^{\text{term}}-C^1$	2.05 Å
		$\angle C^1-C^2-CH_2$	150.6°	$d N^{\text{int}}-C^2$	2.07 Å
		$\angle C^2-C^1-CF_2$	150.0°	$d C\equiv C$	1.26 Å
	BCN (3)	$\angle N_3$	143.0°	$d N^{\text{term}}-C^1$	2.19 Å
		$\angle C^1-C^2-CH_2$	145.8°	$d N^{\text{int}}-C^2$	2.18 Å
		$\angle C^2-C^1-CH_2$	145.2°	$d C\equiv C$	1.25 Å
	DIBO (4)	$\angle N_3$	136.7°	$d N^{\text{term}}-C^1$	2.07 Å
		$\angle C^1-C^2-C$	147.8°	$d N^{\text{int}}-C^2$	2.04 Å
		$\angle C^2-C^1-C$	150.0°	$d C\equiv C$	1.27 Å

Figure 6. (left) TS geometries of **1–4** with allyl azide. (right) Structural data obtained from MP2/6-311G(d,p) optimization.

TS, which probably results in less accurate calculated activation energies. The correlation between the experimental and computational (gas phase) data might even improve further if the experimental data were determined for one solvent system, which is currently not the case (see Table 1). For example, the experimental data for compounds **3**, **4**, and **5** were reported in protic solvents, which are known to speed up the reaction with respect to acetonitrile.^[18] Nevertheless, the high linear correlation found showed that SCS-MP2 data was suitable for use in our envisaged predictive tool. In the remainder of this study we therefore limited ourselves to MP2-optimized geometries and the SCS-MP2 energies thereof.

SPAAC rate constants reported in the literature have mostly been experimentally determined with benzyl azide as the model compound (Table 1). The number of carbon atoms makes the vibrational frequency calculations on the TS of benzyl azide and a cyclooctyne rather time-consuming to track computationally by using Møller–Plesset type calculations. Therefore, we also studied the TS properties with allyl azide, both theoretically and experimentally. Kinetic data on benzyl azide and allyl azide reactivity with **1** were obtained from second-order rate constant experiments. A fivefold excess of a 1:1 mixture of allyl azide and benzyl azide was reacted competitively with **1** in CD₃CN/D₂O (3:1), and, in a separate experiment, with **3**. Because the product ratios of the allyl and benzyl triazole products were 1:1.3 and 1:1.4, respectively (see the Supporting Information), it is clear that the reaction of allyl azide can be compared accurately to that of benzyl azide. This was confirmed computationally: for compounds **1–4** the barriers were computed for both allyl azide and benzyl azide, and the difference between allyl azide and benzyl azide was less than 0.9 kcal mol⁻¹ for all four cases, with the barrier of benzyl azide consistently lower than that of allyl azide (Table 2). Furthermore, the TS geometries for these two systems are highly similar. For example, in the MP2/6-311G(d,p)-derived TS of **1** with benzyl azide, $r(\text{C–N}^{\text{term}})$ and $r(\text{C–N}^{\text{int}})$ are 2.100 and 2.099 Å, respectively, whereas for the allyl azide-derived TS these values are 2.102 and 2.108 Å, respectively (Figure 6). In addition, the imaginary frequencies that track the potential energy curve for approach of the reactants are almost identical (–272.2 and –273.8 cm⁻¹, respectively). Therefore, all TS structures were optimized at the MP2 level of theory for the reaction with allyl azide, whereas for compounds **1–4** these TS structures were also optimized with benzyl azide.

Transition State Geometries

To study the correlation of experimental and theoretical data in more detail, an in-depth study was made of the TS geometries. When comparing the geometrical features of the TS as obtained by the various methods, the TS structures acquired from MP2 calculations were consistently shown to be significantly “tighter” than those obtained from either B3LYP or M06-2X calculations. As a typical

example, Figure 4 shows the relevant bond lengths for the cycloaddition of **1** and allyl azide. With the B3LYP functional, the calculations yielded asymmetric alkyne-azide distances in the order of 2.17–2.31 Å. M06-2X calculations showed near-symmetric distances of approximately 2.20 Å, whereas MP2 calculations showed “tighter” and also near-identical distances of 2.10 Å. In all three cases, **1** adopted a chair-like conformation. In Figure 6, the TS structures of four cyclooctynes, **1–4**, with allyl azide are described as optimized by MP2 calculations; all exhibit a chair-like conformation in the TS with allyl azide. On a first-level approximation, given the exothermic nature of the reaction, lower activation energies could be expected for an earlier TS conformation, in which the C–N distance is larger. This is indeed the case for the TS of **3** with allyl azide, in which the C–N distance is around 2.19 Å, and is more distant in comparison with that in **1** (2.10 Å). Furthermore, in the case of allyl azide and **3**, the azide angle is larger, which means that less N–N–N bending is required to reach the TS conformation. This latter feature is confirmed by the distortion energy of allyl azide (energy difference between the azide in the geometry of the optimized reactant and in the geometry it has in the TS), which is 7 kcal/mol lower than that of allyl azide in a TS with **1** (Table 3). However, for the also more rapidly reacting compound **4**, the TS seems to be later than for **1**. For example, the C–N distances are around 2.05 Å, which implies a tighter TS than found for **1**. This corresponds to the larger distortion energy calculated for the allyl azide and benzyl azide components reacting with **4** in comparison with the reaction with **1** (26.1 and 27.2 kcal/mol for **4**, and 24.8 and 24.4 kcal/mol for **1**, respectively). In other words, although both **3** and **4** also react appreciably faster than **1**, the TS of **3** is characterized by a lower distortion energy, whereas that of **4** is characterized by a higher distortion energy than observed for **1**. A similar discrepancy is observed for **2**, which also reacts faster than **1** but has a later TS (Figure 6). In general, plots of the activation energy versus alkyne or azide distortion energies show only a poor correlation for the studied cyclooctynes (see the Supporting Information, Figure S9). From these observations it can be concluded that the geometries of the TS structures and distortion energies of these cyclooctynes cannot be generally correlated to activating energies of SPAAC reactions. Moreover, natural charges on the alkyne carbon atoms and the azide nitrogen atoms could not be related to the reactivity of the cyclooctynes under study.

Table 3. Distortion energies per component (cyclooctyne or azide) for the SPAAC reactions of cyclooctynes **1–4**, allyl azide (**A**), and benzyl azide (**B**) (in kcal/mol).

Compound	$E_{\text{distortion}}$	Compound	$E_{\text{distortion}}$
1 (+ A)	3.6	A (+ 1)	24.8
1 (+ B)	3.7	B (+ 1)	24.4
2 (+ A)	1.8	A (+ 2)	24.3
2 (+ B)	1.8	B (+ 2)	24.5
3 (+ A)	3.0	A (+ 3)	17.9
4 (+ A)	5.1	A (+ 4)	26.1
4 (+ B)	4.3	B (+ 4)	27.2

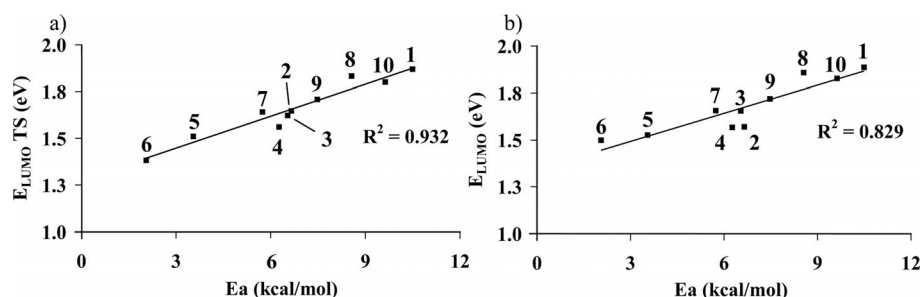


Figure 7. Correlation of the activation energy (in kcal/mol) of the SPAAC transitions states with the LUMO energy (in eV) of cyclooctynes 1–10 (a) in the transition state geometry with allyl azide, or (b) in the geometry they have as a fully optimized reactant.

LUMO Energy Levels as Predictive Tools

In addition to efforts to correlate activation energies to geometrical features of the TS, interactions between the most-involved molecular orbitals were also studied. This revealed a linear correlation between the activation energy E_a and the LUMO energy of the cycloalkyne as it is distorted in the TS (Figure 7, a; $R^2 = 0.932$), which is quite encouraging given the spread of experimental conditions. A lower LUMO energy of the cyclooctyne (in the MP2-calculated TS geometry; please note: MP2 provides an energy correction on Hartree–Fock level-derived orbitals and, as such, the LUMO energy is a Hartree–Fock energy) consistently corresponded to a more rapidly reacting molecule. The HOMO energy of the cyclooctynes could, however, not be related to the activation energy in a convincingly linear fashion (see the Supporting Information, Figure S10). These findings confirm that the SPAAC reaction develops predominantly through azide-HOMO and alkyne-LUMO interactions.^[12,20,31] However, the azide-HOMO energies could also not be related to the SCS-MP2 activation energy ($R^2 = 0.220$; see the Supporting Information, Figure S11). On the contrary, when cyclooctyne LUMO values are correlated to the experimental rate constants, a very good regression is observed ($R^2 = 0.960$; Figure 8). This further supports the idea that the reaction is cyclooctyne LUMO-driven and that Hartree–Fock LUMO values are indeed a good measure for the reactivity of the cyclooctynes in SPAAC reactions with organic azides.

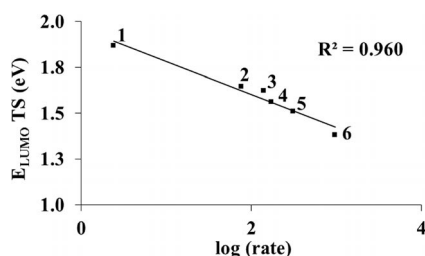


Figure 8. Plot of logarithm of experimental second-order rate constants for cyclooctynes 1–6 vs. the calculated MP2 LUMO energies (in eV) of their geometry in the SPAAC transition state with allyl azide.

Given this success, we wondered whether more simple theoretical tools would be available to rapidly predict the order of reactivity of cyclooctynes in strain-promoted cy-

cloaddition reactions. To this end, we also plotted the LUMO energy of the MP2-optimized cycloalkyne (i.e., full optimization, without presence of azide) against the calculated activation energies (Figure 7, b). This again showed a decent linear correlation ($R^2 = 0.829$), albeit with clearly more scatter than the linear correlation of the LUMO values that was obtained for the cyclooctynes in the transition state. Even this simplified approach yielded the reactivity order $6 > 5 > 4 \approx 3 \approx 2 > 1$, which closely resembles the experimentally observed order $6 > 5 > 4 \approx 3 > 2 > 1$. Even quicker approaches, involving DFT, were less successful ($R^2 = 0.727$ and 0.795 , for B3LYP and M06-2X, respectively) (see the Supporting Information, Figures S12 and S13, respectively). Among the employed methods, only SCS-MP2 is a uniformly robust method that can yield useful SPAAC reactivity predictions. As LUMO energies can be calculated in a straightforward manner in a variety of GUI-assisted molecular simulation programs such as Gaussview or ChemBio3D, this may simplify further experimental optimizations of strain-promoted cycloaddition reactions, possibly also with other dipoles such as nitrones, nitrile oxides,^[18] and other alkynes. A step-by-step standard operating procedure for performing these calculations, thereby giving an indication of the reactivity of novel cyclooctynes in SPAAC reactions, can be found in the Supporting Information.

Conclusions

It is possible to predict the relative reactivity of strained alkynes in SPAAC reactions from the LUMO energy of the alkyne. The LUMO energy in the TS geometry correlates accurately ($R^2 = 0.960$) with the experimental rate order for a diverse series of cyclooctynes. Even the alkyne LUMO energy of the relaxed, fully optimized cyclooctyne yields a good indication of relative reactivities. No good correlation between the experimental rates and alkyne distortion energies was observed. By comparing experimental data with theoretically derived activation energies, it was shown that SCS-MP2 yielded accurate data, but that – although popular – the DFT methods B3LYP and M06-2X did not yield theoretical predictions that correlated favorably with experiment. Given the efficiency and accessibility of basic computational chemistry on 21st century personal computers, the

calculation of LUMO values of novel cyclooctynes on these machines is a rapid and easily available method to obtain an initial valuable estimate of their reaction kinetics in strain-promoted cycloadditions prior to committing to the development of a synthetic route and actually preparing them.

Supporting Information (see footnote on the first page of this article): Experimental procedure for the synthesis of **1** and allyl azide. Determination of rate constants of **1** with benzyl azide. Competition experiment procedure of **1** or **3** with benzyl azide and allyl azide. Plots of E_a (MP2) vs. log rate, TS conformation of **9** and **10**, E_a (SCS-MP2), in: MeOH vs. log rate, E_a (SCS-MP2) vs. cyclooctyne distortion energies, E_a (SCS-MP2) vs. cyclooctyne E_{HOMO} (MP2), E_a (SCS-MP2) vs. allyl azide E_{HOMO} (MP2), E_a (SCS-MP2) vs. cyclooctyne E_{LUMO} (B3LYP), and E_{LUMO} (M06-2X), (SCS-MP2) vs. $E_{\text{HOMO}}(\text{azide}) - E_{\text{HOMO}}(\text{cyclooctyne})$, Table with MO energies of allyl azide and benzyl azide in the TS with compounds **1–10**, step-by-step guideline for the calculation of cyclooctyne rate values.

Acknowledgments

This work is co-financed via the program management Euregio Rhein-Waal by the INTERREG IV, A Germany–Netherlands program through EU funding from the European Regional Development Fund (ERDF), the Ministry for Economic 491 Affairs, Energy, Building, Housing and Transport of the German Federate State of North-Rhine Westphalia and the Dutch Ministry of Economic Affairs and the Province of Gelderland.

- [1] a) T. K. Tiefenbrunn, P. E. Dawson, *Biopolymers* **2010**, *94*, 95–106; b) B. S. Sumerlin, A. P. Vogt, *Macromolecules* **2010**, *43*, 1–13; c) J. C. Jewett, C. R. Bertozzi, *Chem. Soc. Rev.* **2010**, *39*, 1272–1279; d) M. F. Debets, C. W. J. van der Doelen, F. P. J. T. Rutjes, F. L. van Delft, *ChemBioChem* **2010**, *11*, 1168–1184; e) J. M. Baskin, C. R. Bertozzi, *Aldrichim. Acta* **2010**, *43*, 15–23; f) E. M. Sletten, C. R. Bertozzi, *Angew. Chem.* **2009**, *121*, 7108; *Angew. Chem. Int. Ed.* **2009**, *48*, 6974–6998; g) C. R. Becer, R. Hoogenboom, U. S. Schubert, *Angew. Chem.* **2009**, *121*, 4998; *Angew. Chem. Int. Ed.* **2009**, *48*, 4900–4908; h) J. A. Prescher, C. R. Bertozzi, *Nature Chem. Biol.* **2005**, *1*, 13–21.
- [2] a) R. Huisgen, *Angew. Chem.* **1963**, *75*, 604; *Angew. Chem. Int. Ed. Engl.* **1963**, *2*, 565–598; b) C. W. Tornøe, C. Christensen, M. Meldal, *J. Org. Chem.* **2002**, *67*, 3057.
- [3] a) V. V. Rostovtsev, L. G. Green, V. V. Fokin, K. B. Sharpless, *Angew. Chem.* **2002**, *114*, 2708; *Angew. Chem. Int. Ed.* **2002**, *41*, 2596–2599; b) H. C. Kolb, M. G. Finn, K. B. Sharpless, *Angew. Chem.* **2001**, *113*, 2056; *Angew. Chem. Int. Ed.* **2001**, *40*, 2004–2021.
- [4] M. E. Letelier, S. Sánchez-Jofré, L. Peredo-Silva, J. Cortés-Troncoso, P. Aracena-Parks, *Chem.-Biol. Interact.* **2010**, *188*, 220–227.
- [5] a) S. T. Laughlin, C. R. Bertozzi, *ACS Chem. Biol.* **2009**, *4*, 1068–1072; b) J. M. Baskin, K. W. Dehnert, S. T. Laughlin, S. L. Amacher, C. R. Bertozzi, *Proc. Natl. Acad. Sci. USA* **2010**, *107*, 10360–10365; c) S. T. Laughlin, J. M. Baskin, S. L. Amacher, C. R. Bertozzi, *Science* **2008**, *320*, 664–667; d) J. M. Baskin, J. A. Prescher, S. T. Laughlin, N. J. Agard, P. V. Chang, I. A. Miller, A. Lo, J. A. Codelli, C. R. Bertozzi, *Proc. Natl. Acad. Sci. USA* **2007**, *104*, 16793–16797; e) S. T. Laughlin, N. J. Agard, J. M. Baskin, I. S. Carrico, P. V. Chang, A. S. Ganguli, M. J. Hangauer, A. Lo, J. A. Prescher, C. R. Bertozzi, *Methods Enzymol.* **2006**, *415*, 230–250.
- [6] A. T. Blomquist, L. H. Liu, *J. Am. Chem. Soc.* **1953**, *75*, 2153–2154.
- [7] G. Wittig, A. Krebs, *Chem. Ber.* **1961**, *94*, 3260–3275.
- [8] R. B. Turner, A. D. Jarrett, P. Goebel, B. J. Mallon, *J. Am. Chem. Soc.* **1973**, *95*, 790–792.
- [9] N. J. Agard, J. A. Prescher, C. R. Bertozzi, *J. Am. Chem. Soc.* **2004**, *126*, 15046–15047.
- [10] J. M. Baskin, C. R. Bertozzi, *QSAR Comb. Sci.* **2007**, *26*, 1211–1219.
- [11] J. Dommerholt, S. Schmidt, R. P. Temming, L. J. A. Hendriks, F. P. J. T. Rutjes, J. C. M. van Hest, D. J. Lefeber, P. Friedl, F. L. van Delft, *Angew. Chem.* **2010**, *122*, 9612; *Angew. Chem. Int. Ed.* **2010**, *49*, 9422–9425.
- [12] P. König, J. Zountsas, K. Bleckmann, H. Meier, *Chem. Ber.* **1983**, *116*, 3580–3590.
- [13] X. Ning, J. Guo, M. A. Wolfert, G. J. Boons, *Angew. Chem.* **2008**, *120*, 2285; *Angew. Chem. Int. Ed.* **2008**, *47*, 2253–2255.
- [14] E. M. Sletten, H. Nakamura, J. C. Jewett, R. Bertozzi Carolyn, *J. Am. Chem. Soc.* **2010**, *132*, 11799–11805.
- [15] M. F. Debets, S. S. van Berkel, S. Schoffelen, F. P. J. T. Rutjes, J. C. M. van Hest, F. L. van Delft, *Chem. Commun.* **2010**, *46*, 97–99.
- [16] A. Kuzmin, A. A. Poloukhine, M. A. Wolfert, V. V. Popik, *Bioconjugate Chem.* **2010**, *21*, 2076–2085.
- [17] J. C. Jewett, E. M. Sletten, C. R. Bertozzi, *J. Am. Chem. Soc.* **2010**, *132*, 3688–3690.
- [18] X. Ning, R. P. Temming, J. Dommerholt, J. Guo, D. B. Ania, M. F. Debets, M. A. Wolfert, G. J. Boons, F. L. Van Delft, *Angew. Chem.* **2010**, *122*, 3129; *Angew. Chem. Int. Ed.* **2010**, *49*, 3065–3068.
- [19] D. H. Ess, G. O. Jones, K. N. Houk, *Org. Lett.* **2008**, *10*, 1633–1636.
- [20] F. Schoenebeck, D. H. Ess, G. O. Jones, K. N. Houk, *J. Am. Chem. Soc.* **2009**, *131*, 8121–8133.
- [21] R. D. Bach, *J. Am. Chem. Soc.* **2009**, *131*, 5233–5243.
- [22] K. Chenoweth, D. Chenoweth, W. A. Goddard, *Org. Biomol. Chem.* **2009**, *7*, 5255–5258.
- [23] B. Gold, N. E. Shevchenko, N. Bonus, G. B. Dudley, I. V. Alabugin, *J. Org. Chem.* **2012**, *77*, 75–89.
- [24] C. G. Gordon, J. L. Mackey, J. C. Jewett, E. M. Sletten, K. N. Houk, C. R. Bertozzi, *J. Am. Chem. Soc.* **2012**, *134*, 9199–9208.
- [25] a) W. A. van der Linden, N. Li, S. Hoogendoorn, M. Ruben, M. Verdoes, J. Guo, G. J. Boons, G. A. van der Marel, B. I. Florea, H. S. Overkleeft, *Bioorg. Med. Chem.* **2012**, *20*, 662–666; b) P. Van Delft, N. J. Meeuwenoord, S. Hoogendoorn, J. Dinkelaar, H. S. Overkleeft, G. A. Van Der Marel, D. V. Filippov, *Org. Lett.* **2010**, *12*, 5486–5489; c) C. S. McKay, J. A. Blake, J. Cheng, D. C. Danielson, J. P. Pezacki, *Chem. Commun.* **2011**, *47*, 10040–10042; d) N. E. Mbua, J. Guo, M. A. Wolfert, R. Steet, G. J. Boons, *ChemBioChem* **2011**, *12*, 1912–1921; e) I. S. Marks, J. S. Kang, B. T. Jones, K. J. Landmark, A. J. Cleland, T. A. Taton, *Bioconjugate Chem.* **2011**, *22*, 1259–1263; f) I. Singh, F. Heaney, *Chem. Commun.* **2011**, *47*, 2706–2708; g) J. C. M. Van Hest, F. L. Van Delft, *ChemBioChem* **2011**, *12*, 1309–1312; h) F. Friscourt, P. A. Ledin, N. E. Mbua, H. R. Flanagan-Steet, M. A. Wolfert, R. Steet, G.-J. Boons, *J. Am. Chem. Soc.* **2012**, *134*, 5381–5389; i) P. van Delft, E. van Schie, N. J. Meeuwenoord, H. S. Overkleeft, G. A. van der Marel, D. V. Filippov, *Synthesis* **2011**, 2724–2732; j) K. N. Jayaprakash, C. G. Peng, D. Butler, J. P. Varghese, M. A. Maier, K. G. Rajeev, M. Manoharan, *Org. Lett.* **2010**, *12*, 5410–5413; k) K. W. Dehnert, B. J. Beahm, T. T. Huynh, J. M. Baskin, S. T. Laughlin, W. Wang, P. Wu, S. L. Amacher, C. R. Bertozzi, *ACS Chem. Biol.* **2011**, *6*, 548–552; l) N. J. Baumhoyer, M. E. Martin, S. G. Parameswarappa, K. C. Kloepping, M. S. O'Dorisio, F. C. Pigge, M. K. Schultz, *Bioorg. Med. Chem. Lett.* **2011**, *21*, 5757–5761; m) E. M. Sletten, C. R. Bertozzi, *Acc. Chem. Res.* **2011**, *44*, 666–676; n) M. Shelbourne, X. Chen, T. Brown, A. H. El-Sagheer, *Chem. Commun.* **2011**, *47*, 6257–6259; o) I. Singh, C. Freeman, F. Heaney, *Eur. J. Org. Chem.* **2011**, 6739–6746; p) H. Stoeckmann, A. A. Neves, S. Stairs, H. Ireland-Zecchini, K. M. Brindle, F. J. Leeper, *Chem. Sci.* **2011**, *2*, 932–936; q) V. Bouvet, M. Wuest,

- F. Wuest, *Org. Biomol. Chem.* **2011**, *9*, 7393–7399; r) A. Bernardin, A. Cazet, L. Guyon, P. Delannoy, F. Vinet, D. Bonnaffé, I. Texier, *Bioconjugate Chem.* **2010**, *21*, 583–588; s) L. A. Canalle, M. Van Der Knaap, M. Overhand, J. C. M. Van Hest, *Macromol. Rapid Commun.* **2011**, *32*, 203–208; t) C. Ornelas, R. Lodescar, A. Durandin, J. W. Canary, R. Pennell, L. F. Liebes, M. Weck, *Chem. Eur. J.* **2011**, *17*, 3619–3629; u) L. A. Canalle, T. Vong, P. H. H. M. Adams, F. L. Van Delft, J. M. H. Raats, R. G. S. Chirivi, J. C. M. Van Hest, *Biomacromolecules* **2011**, *12*, 3692–3697; v) G. de Almeida, E. M. Sletten, H. Nakamura, K. K. Palaniappan, C. R. Bertozzi, *Angew. Chem.* **2012**, *124*, 2493; *Angew. Chem. Int. Ed.* **2012**, *51*, 2443–2447; w) R. van Geel, G. J. M. Pruijn, F. L. van Delft, W. C. Boelens, *Bioconjugate Chem.* **2012**, *23*, 392–398; x) F. Friscourt, C. J. Fahrni, G.-J. Boons, *J. Am. Chem. Soc.* **2012**, *134*, 18809–18815; y) J. Z. Yao, C. Uttamapinant, A. Poloukhine, J. M. Baskin, J. A. Codelli, E. M. Sletten, C. R. Bertozzi, V. V. Popik, A. Y. Ting, *J. Am. Chem. Soc.* **2012**, *134*, 3720–3728.
- [26] a) R. K. Manova, S. P. Pujari, C. A. G. M. Weijers, H. Zuilhof, T. A. v. Beek, *Langmuir* **2012**, *28*, 8651–8663; b) R. K. Manova, T. A. van Beek, H. Zuilhof, *Angew. Chem.* **2011**, *123*, 5540; *Angew. Chem. Int. Ed.* **2011**, *50*, 5428–5430.
- [27] C. Lee, W. Yang, R. G. Parr, *Phys. Rev. B* **1988**, *37*, 785.
- [28] Y. Zhao, D. G. Truhlar, *Acc. Chem. Res.* **2008**, *41*, 157.
- [29] a) C. Möller, M. S. Plesset, *Phys. Rev.* **1934**, *46*, 618; b) S. Grimme, *J. Chem. Phys.* **2003**, *118*, 9095.
- [30] M. J. Frisch, G. W. Trucks, H. B. Schlegel, G. E. Scuseria, M. A. Robb, J. R. Cheeseman, G. Scalmani, V. Barone, B. Mennucci, G. A. Petersson, H. Nakatsuji, M. Caricato, X. Li, H. P. Hratchian, A. F. Izmaylov, J. Bloino, G. Zheng, J. L. Sonnenberg, M. Hada, M. Ehara, K. Toyota, R. Fukuda, J. Hasegawa, M. Ishida, T. Nakajima, Y. Honda, O. Kitao, H. Nakai, T. Vreven, J. A. Montgomery Jr., J. E. Peralta, F. Ogliaro, M. Bearpark, J. J. Heyd, E. Brothers, K. N. Kudin, V. N. Staroverov, R. Kobayashi, J. Normand, K. Raghavachari, A. Rendell, J. C. Burant, S. S. Iyengar, J. Tomasi, M. Cossi, N. Rega, J. M. Millam, M. Klene, J. E. Knox, J. B. Cross, V. Bakken, C. Adamo, J. Jaramillo, R. Gomperts, R. E. Stratmann, O. Yazyev, A. J. Austin, R. Cammi, C. Pomelli, J. W. Ochterski, R. L. Martin, K. Morokuma, V. G. Zakrzewski, G. A. Voth, P. Salvador, J. J. Dannenberg, S. Dapprich, A. D. Daniels, Ö. Farkas, J. B. Foresman, J. V. Ortiz, J. Cioslowski, D. J. Fox, *Gaussian 09*, rev. A.02, Gaussian, Inc., Wallingford CT, **2009**.
- [31] I. Fleming, *Molecular Orbitals and Organic Chemical Reactions*, Student Edition John Wiley & Sons, New York, **2010**.

Received: December 3, 2012

Published Online: ■